Quarterly Reviews of Biophysics

www.cambridge.org/qrb

Structural biology inside multicellular specimens using electron cryotomography

Ido Caspy, Zhexin Wang and Tanmay A.M. Bharat

Structural Studies Division, MRC Laboratory of Molecular Biology, Cambridge, UK

Review

Cite this article: Caspy I, Wang Z and Bharat TAM (2025). Structural biology inside multicellular specimens using electron cryotomography. *Quarterly Reviews of Biophysics*, **58**, e6, 1–13
https://doi.org/10.1017/S0033583525000010

Received: 21 October 2024
Revised: 30 December 2024
Accepted: 01 January 2025

Keywords:
cryo-EM; cryo-ET; FIB-SEM; focused ion beam milling; *in situ* imaging; structural biology; subtomogram averaging; tissue ultrastructure; vitrification; volume imaging

Corresponding author:
Tanmay A.M. Bharat;
Email: tbharat@mrc-lmb.cam.ac.uk

Abstract

The electron cryomicroscopy (cryo-EM) resolution revolution has shifted structural biology into a new era, enabling the routine structure determination of macromolecular complexes at an unprecedented rate. Building on this, electron cryotomography (cryo-ET) offers the potential to visualise the native three-dimensional organisation of biological specimens, from cells to tissues and even entire organisms. Despite this huge potential, the study of tissue-like multicellular specimens via cryo-ET still presents numerous challenges, wherein many steps in the workflow are being developed or in urgent need of improvement. In this review, we outline the latest techniques currently utilised for *in situ* imaging of multicellular specimens, while clearly enumerating their associated limitations. We consider every step in typical workflows employed by various laboratories, including sample preparation, data collection and image analysis, to highlight recent progress and showcase prominent success stories. By considering the entire structural biology workflow for multicellular specimens, we identify which future exciting developments in hardware and software could enable comprehensive *in situ* structural biology investigations, bringing forth a new age of discovery in molecular structural and cell biology.

Table of contents

Introduction

The electron cryomicroscopy (cryo-EM) resolution revolution launched structural biology into a time of unprecedented discovery, making it possible to routinely solve structures of purified macromolecular complexes at an astonishing rate (Henderson, 2004; Kühlbrandt, 2014; McCafferty et al., 2024; Nogales & Scheres, 2015). This quantum leap has set the stage for another advance where structural biology questions could be posed directly within the native, three-dimensional (3D) environment of biological specimens that range from organelles to single cells, up to tissues and whole organisms using electron cryotomography (cryo-ET) (Baumeister et al., 1999; Frank, 1995; McCafferty et al., 2024; Nogales & Mahamid, 2024). Using cryo-ET, the intricate cellular environment can now be visualised at the nanometre scale (Beck & Baumeister, 2016; Gan & Jensen, 2012).

In cryo-ET, a series of two-dimensional (2D) images of a vitrified biological sample is acquired at various tilt angles, termed tilt-series. Images in such tilt-series are subsequently aligned and computationally combined to produce a 3D reconstruction of the specimen, which is called a tomogram (Baumeister, 2005; De Rosier & Klug, 1968; Hoppe, 1970, 1974). Each tomogram holds within it a veritable treasure-trove of data, containing information about the molecular composition of the specimen along with its ultrastructural arrangement (Melia & Bharat, 2018; Singh et al., 2024; Xue et al., 2022; P. Zhang, 2019; Zimmerli et al., 2021).

While cryo-ET has been applied to a wide variety of specimens, there are still several difficulties associated with investigating multicellular specimens with this technique. These difficulties are specifically related to vitrification of thick specimens, sample thinning, as well

as subsequent challenges in cryo-ET data acquisition and image processing. These difficulties will be addressed in turn in this article, along with some recent success stories and a balanced reflection on the future applicability of cryo-ET for near-native imaging of tissues.

Sample preparation methods

A requirement to visualise biological specimens using cryo-ET (or cryo-EM) is that the specimen must be vitrified, meaning that the aqueous environment of the specimen of interest should form an amorphous, glass-like arrangement (Dubochet & McDowall, 1981; McDowall et al., 1983). Vitrification preserves the sample in a near-native state, providing ideal conditions for imaging while minimising radiation damage, with no artefacts in imaging caused by crystalline ice, by avoiding electron diffraction from ice crystals that corrupt the acquired data (Dubochet et al., 1988; Henderson, 1992). It is worth mentioning that while vitrification has been deemed as a necessity for cryo-EM, recent work has demonstrated reduction in beam induced motion and better reconstructions from the initial frames of the movie acquisition in a specimen devitrified in a controlled manner (Wieferig et al., 2021). Nonetheless, to prepare a suitably vitrified sample, the specimen must be cooled at a rate faster than the rate of crystalline ice formation (Dubochet et al., 1988). While most biological specimens are present in an aqueous solution, the peculiarities of each individual specimen being studied in any particular experiment determines how, practically, vitrification is performed to ensure suitable preservation for cryo-ET. Broadly, there are two major techniques that can be utilised to produce a vitrified sample – plunge freezing for thin specimens, up to ~10 μm in thickness (Fuest et al., 2019), and high-pressure freezing (HPF) for thicker specimens. For both plunge frozen and high-pressure frozen samples, the quality of vitrification must be investigated experimentally (for instance, by using electron diffraction), as this cannot be reliably assumed *a priori*, because vitrification intimately depends on the chemical characteristics of the sample.

Vitrification of thin samples

The conventional method of specimen vitrification for single-particle cryo-EM is to plunge the specimen into a cryogen such as liquid ethane (Bock & Grubmüller, 2022; Dubochet et al., 1988). Liquid ethane at −180 °C can generate a cooling rate of 10^6 °C/s (Dubochet et al., 1988), thereby allowing a layer of water, generally thinner than 500 nm, to be rapidly vitrified in less than 100 μs, before the volume of the water can expand and crystalline ice of any form can manifest itself. During plunge freezing, the biological sample is applied onto a cryo-EM grid (Schaffer et al., 2017), followed by wicking the excess liquid off, to leave a thin film of the specimen on the grid, which is then plunged into the cryogen. Alternatively, cells may be grown directly on cryo-EM grids, often after the grid is coated with polymers such as poly-L-lysine or fibronectin that aid cellular adherence to the grid surface (Lam & Villa, 2021; Mahamid et al., 2016; F. R. Wagner et al., 2020). Due to the high heat capacity of the cryogen, the sample is cooled at a rapid rate, leading to efficient vitrification (Dubochet & McDowall, 1981). Additionally, samples can also be vitrified using a cryogen stream (Ravelli et al., 2020), dispensed onto a grid in minute volumes and at rapid intervals designed principally for time sensitive specimens (Dandey et al., 2020), or cryofixed during light-microscope imaging using a correlative light and electron microscope (CLEM) fitted with a microfluidics device (Fuest et al., 2019). Even more excitingly, protein samples can be passed through a mass spectrometer in a gaseous state and deposited on a cryo-cooled grid for cryo-EM, allowing an accurate characterisation of the applied specimen prior to imaging (Esser et al., 2024). These approaches offer a lot of flexibility in the sample preparation of biological material. However, for *in situ* imaging of cells and tissues, all the approaches discussed thus far are limited to relatively thin specimens, because the cooling rate drastically drops at locations away from the surface of the specimen. The thickness limitation for vitrification at ambient atmospheric pressure is around 10 μm, although it varies between different biological specimens and can be slightly circumvented by the addition of cryoprotectants (Bäuerlein et al., 2023; Berger, Premaraj, et al., 2023; Fuest et al., 2019; Jentoft et al., 2023; F. R. Wagner et al., 2020).

Vitrification of thick samples

An alternative to the approaches listed above for thin specimens is available, termed high-pressure freezing (HPF), which was developed several decades ago (Moor & Riehle, 1968), and is particularly suitable for thicker samples up to ~200 μm (Kelley et al., 2022; Studer et al., 2008). During HPF, a pressure of ~2100 bar is applied to biological specimens clasped between two metal planchettes during freezing. As ice is less dense than water, the high pressure hinders crystalline ice formation, thereby reducing the cooling rate requirement for vitrification (Moor, 1987). To further prevent crystalline ice from forming and improve vitrification, a cryoprotectant can be added to the sample such as glycerol (Dahl & Staehelin, 1989), glycans (I. Y. Chang et al., 2021), polyvinyl compounds (Weil et al., 2019) and 1-hexadecene (McDonald et al., 2010). These cryoprotectants prevent the formation of crystalline ice by increasing the global concentration of all solutes present in the aqueous sample (Pegg, 2007). Another special cryoprotectant is 2-methylpentane, which can be sublimed from the vitrified specimen by heating to −150 °C, allowing additional advantages such as post-addition of fiducials, as well as for exposing the surface topography of specimens to reduce the volume that needs to be removed in the downstream thinning step (Harapin et al., 2015; S. Wang et al., 2023).

Another route to accessing thicker volumes is to use the so-called waffle method (Figure 1a) following earlier reports of a similar nature (Weiner et al., 2013), where a grid is sandwiched between two planchettes and high-pressure frozen using the grid bars as a spacer (Kelley et al., 2022). This approach is designed to accommodate various samples at a thickness compatible with maximal reasonable gallium milling depth, which is ~50 μm (Schaffer et al., 2019). This approach is applicable to cellular or multicellular samples, sometimes made possible by concentrating the cells (by skipping blotting), thus circumventing preferred orientation of the cells, and could be useful for purified particles as well (Kelley et al., 2022).

Yet even HPF is limited by the sample thickness and is typically useful only up to 100–200 μm (Kelley et al., 2022; Studer et al., 2008). Accessing thick tissues is currently made possible by initial mechanical sectioning using a vibratome prior to vitrification. Typically, the sample is immersed in buffer or embedded in agar, then sliced using a blade and placed on a grid for HPF (Creekmore et al., 2024; Matsui et al., 2024; J. Zhang et al., 2021). However, this step prolongs the period between sample isolation and freezing and can introduce cutting artefacts at the surface of the sample, which could hinder the preservation of the native, physiologically relevant

https://doi.org/10.1017/S0033583525000010 Published online by Cambridge University Press

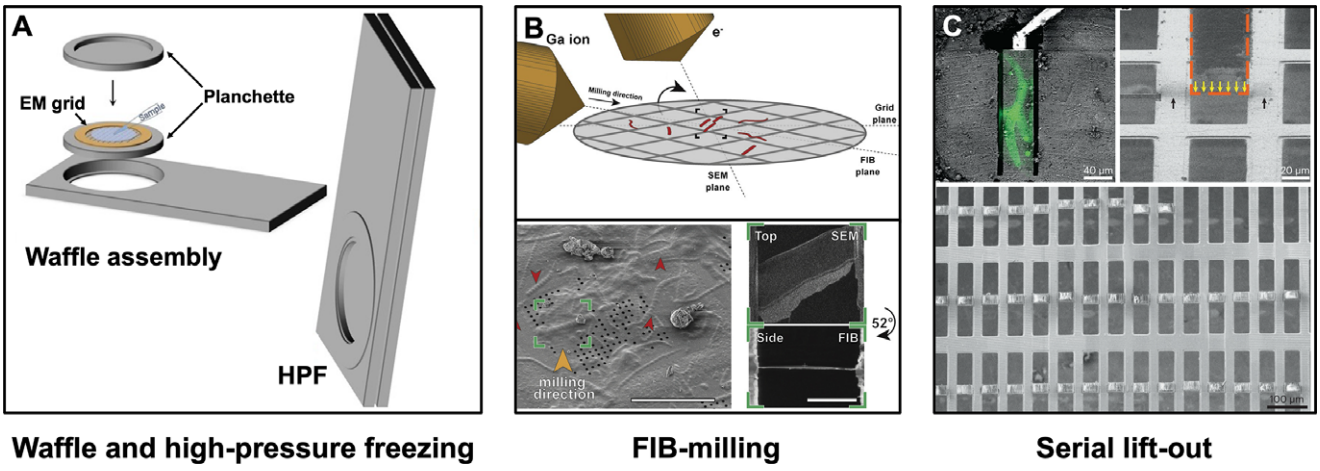

Figure 1. Overview of sample preparation by HPF and FIB milling of cellular and tissue specimens. (a) Cartoon description of the waffle assembly – the EM grid is placed between two planchettes and subsequently vitrified using HPF. Adapted from Kelley et al. (2022). Image is CC BY, license link: http://creativecommons.org/licenses/by/4.0/. (b) Schematic showing the geometry of the focused ion beam, SEM and the grid containing the sample (top). SEM image of a plunge-frozen sample with the milling direction marked, and myofibrils are marked with red arrows (bottom left). Polished lamella images, top-view imaged with the SEM, and side-view imaged with the FIB (bottom right). Bottom left scale bar 50 µm; Bottom right panel 5 µm. Adapted from Z. Wang et al. (2021). (c) Serial lift-out workflow: After the region of interest was identified using fluorescent labelling (green), the micromanipulator was mounted, and the area was milled in preparation for lift-out (top left). The slab removed in the previous step is positioned for subsequent thinning (top right). Overview of the milled sections prior to cryo-ET data collection (bottom). Adapted from Schiøtz et al. (2023). Image is CC BY, license link: http://creativecommons.org/licenses/by/4.0/.

state of interest. Thus, at the sample preparation stage, there is an urgent need to develop novel techniques for obtaining vitrified samples of much larger volumes, in particular when aiming to image entire tissues and organisms (Baumeister, 2005; Hutchings & Zanetti, 2018).

Thinning procedures

For cryo-ET data acquisition, since the electrons must be transmitted through the biological specimen, to be able to contribute to image formation at the detector, the mean free path of electrons, or removal of inelastically scattered electrons by an energy filter, limits specimen thickness usable for cryo-ET. This thickness limit has been estimated by different studies that reported slightly different values, with some studies reporting this limit to be as low as 300 nm, because the effective thickness of the specimen increases significantly at high tilt angles during cryo-ET data acquisition, and the signal-to-noise ratio is thus greatly diminished (Petrov et al., 2022). Even for a 200 nm-thick specimen, it has been reported that the total transmitted electrons are roughly half of the illuminated dose, as they interact with the sample resulting in decoherence and energy loss (Elbaum, 2018). As most cellular specimens, apart from a few examples of smaller microbial cells (O'Reilly et al., 2020; von Kügelgen et al., 2024), are usually thicker than 200–300 nm (Melia & Bharat, 2018; Oikonomou et al., 2016), they must be thinned before cryo-ET can be performed. Previously, sample thinning for cryo-EM was only possible using cryo-ultramicrotomy, where a diamond knife is used to produce thin sections of the specimen at cryogenic temperatures. These sections are subsequently placed on an EM grid for imaging (Al-Amoudi et al., 2004; Bharat et al., 2018; Eltsov et al., 2018; Gilbert et al., 2024; Leistner et al., 2023; McDowall et al., 1983). This method, termed cryo-electron microscopy of vitrified sections (CEMOVIS), might lead to distortions in the specimen including expansion and compression due to the mechanical action of the knife. Even though CEMOVIS can be used successfully to study cellular and tissue samples *in situ* (Bharat et al., 2018; Gilbert et al., 2024; Ma et al., 2022), practical application of CEMOVIS tends to be quite tedious as the sample is prepared manually with low throughput, with the skill of the experimentalist critically determining the outcome of the procedure (Al-Amoudi et al., 2005).

Thinning of thin(ner) specimens using ion beams

To bypass this limitation of CEMOVIS, focused-ion-beam milling (FIB milling) was adapted from material sciences and applied to biological specimens at cryogenic temperatures to obtain thin samples amenable for cryo-ET with minimal artefacts (Marko et al., 2006, 2007; Rigort, Bäuerlein, et al., 2012; Rigort, Villa, et al., 2012). For a comprehensive overview of the technique, we recommend other authoritative reviews (Noble & de Marco, 2024; Rigort & Plitzko, 2015). In brief, a focused ion beam, such as one containing gallium metal ions, is utilised to ablate biological material and mill it down to a lamella with a final thickness of roughly 180–200 nm (Villa et al., 2013). Before milling, the vitrified specimen is typically coated with a layer of organometallic platinum compound to protect the sample surface and to ensure that the milling process results in a smooth lamella (Schaffer et al., 2017). During milling, high gallium currents (500–1000 pA) are initially used to remove bulk materials and expose the central segment of the specimen containing the region of interest. As high currents can introduce damage to the specimen, in subsequent steps, the ion current is progressively reduced and the sample is gradually milled and polished, resulting in a thin, uniform lamella that is amenable for cryo-ET (Figure 1b; Rigort, Bäuerlein, et al., 2012; Schaffer et al., 2017; F. R. Wagner et al., 2020). Recent studies aimed at characterising the extent of the radiation damage introduced to lamellae by the ion beam estimated that the specimen up to 30–60 nm in depth from the lamella surface is affected by milling with gallium ions (Lucas & Grigorieff, 2023; Tuijtel et al., 2024). Moreover, the data showed that lamellae thinner than 180 nm do not offer any significant improvement in the resolution obtained after subtomogram averaging, likely due to the radiation damage (Tuijtel et al., 2024). This is especially noteworthy since many groups aim for lamella thickness of 100–120 nm. In comparison, for cryo-EM SPA, the ideal ice thickness has been proposed to be as small as 30 nm (Koeck

https://doi.org/10.1017/S0033583525000010 Published online by Cambridge University Press

& Karshikoff, 2015), although 3 Å resolution could be achieved with ice as thick as 200 nm (Neselu et al., 2023).

Thinning of thick specimens using FIB milling

FIB milling using gallium beams is widespread, allowing the precise generation of lamellae. The drawback is that gallium thinning is a relatively slow process, since high currents are not achievable with the available hardware configurations of the liquid metal ion sources (Burnett et al., 2016). As a result, milling specimens thicker than 50 µm is challenging. The solution is to employ different milling strategies, use more powerful beams, or a combination of both, which will be discussed in this section. To access regions far from the tissue surface for structural studies using cryo-ET, a method termed lift-out has been developed (Mahamid et al., 2015; Rubino et al., 2012; Schaffer et al., 2019). Classical FIB-milling requires the removal of most of the material around the region-of-interest. Lift-out employs a micromanipulator with a needle or gripper at its tip to lift-out a slab that is cut off the specimen by FIB, thereby reducing the amount of material needed to be removed, in order to access deep regions. This lift-out technique is becoming more widely applied, as it allows detailed inspection of complex 3D tissue or even whole organisms in their native context. Recently, a serialised lift-out approach which produces multiple lamellae within one lift-out process has been developed to improve the throughput (Figure 1c; Gilbert et al., 2024; Klumpe et al., 2022, 2023; Kuba et al., 2021; Nguyen et al., 2024; Plitzko et al., 2022; Schiøtz et al., 2023; Zens et al., 2024).

An alternative to using a gallium ion beam is the use of various gaseous ions produced from plasma (Berger, Dumoux, et al., 2023; Zhong et al., 2021). Plasma sources can deliver higher currents (Burnett et al., 2016; Gorelick & Marco, 2018; Lai et al., 2017), albeit with reduced precision, which permit milling of larger volumes when compared to liquid metal sources (Berger, Dumoux, et al., 2023; Burnett et al., 2016; Chang et al., 2019; Dumoux et al., 2023; Eder et al., 2021; Parkhurst et al., 2023). Thorough examination and analysis are still required to elucidate the relative advantages of using plasma sources over liquid metal ion sources, and which gases are optimal for use in the thinning and polishing steps of lamellae preparation. Current data suggest beams using xenon plasma sources can dispose of material at a faster rate than gallium beams, suggesting that they could be useful during the rough milling step of large volumes, while argon produces lamellae at a high success rate with relatively lower radiation damage (Berger, Dumoux, et al., 2023; Berger et al., 2024; Burnett et al., 2016). When the specimen is too thick to be thinned using FIB-milling (in the case of large organs or organisms), performing a mechanical thinning step using a vibratome and/or and an ultramicrotome presents an alternative approach to obtain a sample amenable for downstream milling (Creekmore et al., 2024; Iulianella, 2017; Matsui et al., 2024; McCafferty et al., 2024; S. Wang et al., 2023; J. Zhang et al., 2021). In the future ideally, larger areas of vitrified grids would be thinned using ion beams, making entire tissues and organisms amenable for cryo-ET data acquisition.

Various approaches in the field are currently aimed at turning cryo-FIB milling into a fully automated process, rescinding the need for high user proficiency, thus making it possible to generate more than ~50 lamellae in a single session. Hardware improvements such as the installation of cryo-shields, obtaining better chamber vacuum systems and attempts to integrate the FIB platform with TEMs to reduce contamination, all together improve the stability of the lamellae produced and increase the throughput of sample preparation for cryo-ET (Berger, Premaraj, et al., 2023; Cleeve et al., 2023; Klumpe et al., 2021; Medeiros et al., 2018; Tacke et al., 2021; Zachs et al., 2020). Future EM setups will likely include all modules present in the same type of sample holder compatible with cryo-FIB-SEM and TEM with the data collection software keeping track of the grid locations throughout the process. This will go a long way to making sample preparation and data collection more efficient, less prone to human error and with reduced contamination. Some modified setups are already available, such as the additional accessory fluorescent light-microscopes (J. Yang et al., 2023), and future setups may include mass spectrometers that could assist in localised targeting and on-the-fly compositional analysis of the specimen (Esser et al., 2024; Lindell et al., 2024; Passarelli et al., 2017).

Cryo-ET of thinned specimens

Once the multicellular specimen has been appropriately thinned, it is ready for cryo-ET data collection for structural and cell biology. One of the major factors limiting the throughput of cryo-ET is the long acquisition time of tilt-series, compared to cryo-EM single particle analysis (Böhning & Bharat, 2021). Different data collection schemes have sought to overcome this hurdle to support widespread application of cryo-ET. One such approach accelerates the speed of a single tilt-series acquisition by implementing a continuous data collection (Chreifi et al., 2019, 2021; Eisenstein et al., 2019). In this scheme, the specimen is exposed and tilted continuously (in a single movement) without the need to track and correct stage shifts, required in standard cryo-ET data collection (Mastronarde, 2005). Abandoning these constant adjustments, which require slow mechanical stage movements in the microscope, increases the speed of tilt-series acquisition up to an order of magnitude, but limits the overall quality of the reconstructed tomograms since the tilt angle of each image must be estimated experimentally (Chreifi et al., 2019). Other approaches aimed at optimally imaging each square nanometre of the valuable milled area of the specimen include the use of overlapping tiles that are stitched together, thereby forming mosaic images that can eventually be merged and reconstructed as a highly detailed, large tomographic volume (Peck et al., 2022). Alternatively, the beam shape could be changed to a square to maximise the collection area within the lamella and permit data acquisition of neighbouring areas without losing high-resolution features due to overlapping, unnecessary exposure during data collection (Brown et al., 2024; Chua et al., 2024).

Perhaps the most widely applicable acquisition strategy parallelises cryo-ET data collection by defining a geometric model describing the lamella surface (or any specimen surface) relative to the tilt axis. This geometric model helps in parallelised data collection by utilising beam image shifts combined with a single tracking area, hence allowing multiple tilt-series acquisition in a nearly simultaneous manner. This facilitates the collection of hundreds of tilt series in a single session, substantially increasing throughput compared to the traditional collection schemes (Bouvette et al., 2021; Eisenstein et al., 2022; J. E. Yang et al., 2023). To overcome errors introduced either by misaligned lamellae, specimen rotation caused by the mechanical autoloader system, and inaccurate measurement of the lamella's eucentric position, the geometric model is used to compensate for these errors and is updated throughout sample tilting in the PACE-tomo (parallel cryo electron tomography) workflow (Figure 2a; Eisenstein et al., 2022). To complement this approach and introduce further automation, a machine learning

https://doi.org/10.1017/S0033583525000010 Published online by Cambridge University Press

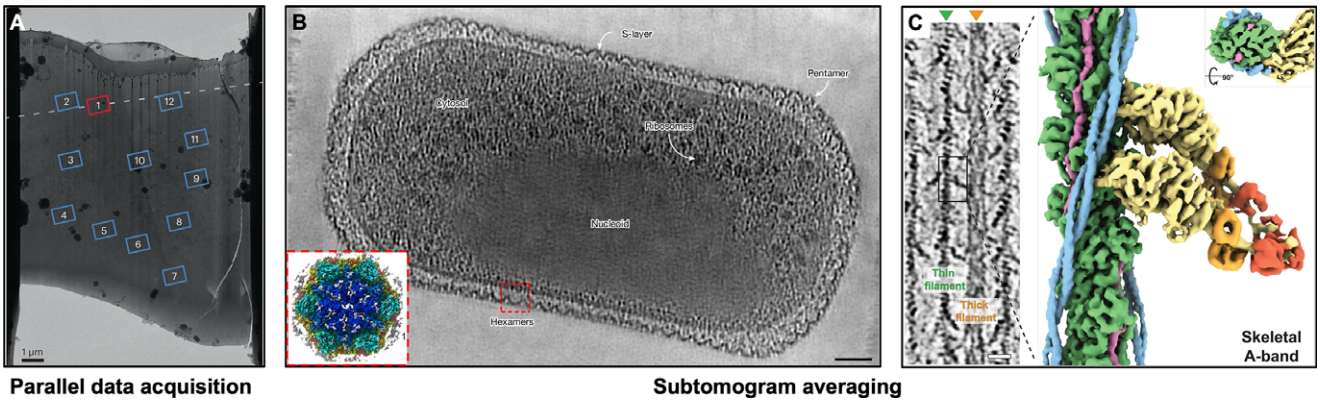

Figure 2. Cryo-ET data collection and high resolution subtomogram averaged structures. (a) FIB-milled lamella with defined regions for parallel cryo-ET data acquisition using beam image shifts. The tilt axis is marked with a dashed line. Adapted from Eisenstein et al. (2022). Reproduced with permission from SNCSC. (b) Slice through a tomogram of an entire microbial cell where ribosomes, nucleoid and the surface layer (S-layer) encapsulating the cell are all visible. Inset - the subtomogram averaged map of the S-layer, scale bar 50 nm. Adapted from von Kügelgen et al. (2024). Image is CC BY, license link: http://creativecommons.org/licenses/by/4.0/. (c) Slice through a tomogram of the sarcomere thin and thick filaments along with the subtomogram averaged map of the thin filament with a bound myosin. Scale bar 20 nm. Adapted from Z. Wang et al. (2022). Reprinted with permission from AAAS.

model dubbed SPACE-tomo (smart parallel automated cryo electron tomography) was trained to facilitate unattended lamella definition, identification and segmentation of regions of interest within the lamella, and data acquisition set-up (Eisenstein et al., 2023). As these methods become more widespread, we expect that such unsupervised approaches will become an indispensable part of the cryo-ET data collection pipelines.

While cryo-ET data collection has advanced significantly since the advent of direct electron detectors, there is still room to substantially improve the quality of cryo-ET data, which will potentially have a huge impact on reducing the amount of data needed to solve structures inside cells and tissues. Lamella preparation requires a lot of time and effort; therefore, it is imperative that the cryo-ET data collected is of the highest possible quality (Ochner & Bharat, 2023). From a hardware standpoint, the laser phase plate is drawing significant attention and holds the potential to substantially improve the signal-to-noise ratio in cryo-ET by modulating the phase contrast difference between scattered and unscattered electrons, during in-focus specimen imaging (Müller et al., 2010). The unscattered electrons are focused and passed through an electric field generated by an ultrafast continuous (Schwartz et al., 2019) or pulsed (Du & Fitzpatrick, 2023) laser. The passage through the field induces a phase shift caused by the ponderomotive force, resulting in a phase difference ($\pi/2$ in the case for a quarter phase plate), thus boosting contrast significantly even when the specimen is in focus (Du & Fitzpatrick, 2023; Müller et al., 2010; Schwartz et al., 2019). The phase contrast of the detected electrons results in better image quality by converting the sine oscillation to cosine, thus increasing the low-frequency signal, although CTF correction is still required for both low and high resolution (Campbell et al., 2018; Müller et al., 2010; Petrov et al., 2022; Schwartz et al., 2019). The drawback of the current design was described as a resolution loss due to magnetic field fluctuations caused by the laser pulses, which are currently being investigated for future improvements (Axelrod, Petrov, Zhang, Remis, et al., 2023; Axelrod, Petrov, Zhang, Sandhaus, et al., 2023).

Subtomogram averaging structure determination

Once cryo-ET data on the multicellular specimen has been collected, subtomogram averaging (STA) can be applied to obtain structural information from the macromolecules present within the specimen. Subtomogram averaging approaches have been described in other reviews focused on this method (Briggs, 2013; Lučić et al., 2013); therefore, it is only considered here briefly for completeness. Following tilt-series acquisition, tomograms can be reconstructed in a variety of software (Kremer et al., 1996; Zheng et al., 2022) using a variety of pipelines (Burt et al., 2024; Himes & Zhang, 2018; H. F. Liu et al., 2023). Next, typically tomographic volumes are denoised to improve contrast (Buchholz et al., 2018; Y. T. Liu et al., 2022), after which researchers can use a variety of tools for manual picking, template matching or other feature identification tasks (Chaillet et al., 2024; Cruz-León et al., 2024; de Teresa-Trueba et al., 2023; Lucas et al., 2023; Moebel et al., 2021; Rice et al., 2023; T. Wagner et al., 2019, 2020; Wan et al., 2024). These subtomogram selection tasks can be followed by classification and subtomogram averaging (Burt et al., 2024; M. Chen et al., 2019; Förster et al., 2005; H. F. Liu et al., 2023; Tegunov et al., 2021). Subtomogram averaging allows structure determination of macromolecules in their native environment (Figure 2b-c; Allegretti et al., 2020; S. Chen et al., 2024; Z. Chen et al., 2023; Fedry et al., 2024; Gemmer et al., 2023; Q. Guo et al., 2018; Held et al., 2024; Hoffmann et al., 2022; Hutchings et al., 2018; Kravčenko et al., 2024; Leung et al., 2023; Mattei et al., 2016; Ni et al., 2022; Obr et al., 2024; Pyle et al., 2024; Santos et al., 2024; Schur et al., 2016; Tamborrini et al., 2023; Turoňová et al., 2020; von Kügelgen et al., 2020, 2024; J. Wagner et al., 2024; Waltz et al., 2024; Z. Wang et al., 2021, 2022; Watanabe et al., 2020, 2024; Wozny et al., 2023; Xue et al., 2022; You et al., 2023; X. Zhang et al., 2023; Zimmerli et al., 2021), using image processing algorithms that support high-resolution structure determination (Bharat et al., 2015; Burt et al., 2024; Tegunov et al., 2021; Zivanov et al., 2022). The resulting structures provide valuable insights on the mode of action of macromolecules in tissues, along with their interactions with drugs, ligands, or accessory molecules *in situ*. These interactions are often transient or disrupted by protein purification techniques and thus cannot be easily reconstituted and visualised *in vitro*.

Several modern studies not only report the cellular structures of macromolecules by STA but also map the resulting structures back into the original tomogram, providing additional ultrastructural information of the tissue. With this in mind, we must note that a thinned sample is taken out of the cellular or tissue context, because

https://doi.org/10.1017/S0033583525000010 Published online by Cambridge University Press

once thinned, it represents only a small slice from the initial intact specimen. We anticipate that in the next few years, more molecular structures will be characterised using a workflow combining cryo-FIB-SEM, cryo-ET, predictive algorithms (Jumper et al., 2021) and cellular transcriptomics and proteomics approaches (Baumeister, 2005; McCafferty et al., 2024).

Complementary techniques for 3D *in situ* imaging

Cryo-ET provides molecular resolution in a limited sample volume, due to the requirement of thinning tissue specimens. This limitation can be partially alleviated by montage tomography (Peck et al., 2022; J. E. Yang et al., 2023), which expands the field-of-view in the "X-Y" dimension, and by serial lift-out approaches, which increases depth through fabrication of multiple lamellae from the same tissue (Nguyen et al., 2024; Schiøtz et al., 2023). However, this loss of sample volume due to thinning is to an extent unavoidable in cryo-ET. To circumvent this issue, there are other *in situ* imaging techniques that provide an alternative option for imaging bulk volumes such as 3D FIB-SEM imaging (also termed serial surface imaging or "slice-and-view"), where a layer of biological material is removed using the FIB followed by imaging of the exposed surface using the SEM. By iterating the FIB-SEM process, a 3D volume can be generated with a nearly isotropic resolution of a few nanometres. This technique is extremely useful for cell biological investigations inside tissues, because it provides a large field-of-view, and depth information through the "Z"-axis of the tissue (Elbaum, 2018). This serial FIB-SEM technique had previously been widely applied for room temperature specimens that were chemically fixed (Denk & Horstmann, 2004; D'Imprima et al., 2023; Heymann et al., 2006; Xu et al., 2017, 2021) and has been recently expanded to cryogenic temperature applications (Capua-Shenkar et al., 2022; Scher et al., 2021; Schertel et al., 2013; Sviben et al., 2016; Vidavsky et al., 2015, 2016). Despite the large potential applications, several challenges remain in the pipeline for imaging cryogenic, unstained biological specimen, such as problems with automatic focusing, automatic astigmatism and drift correction on these radiation sensitive samples that are imaged for several hours, and sometimes several days. Moreover, interpretation of the resulting images remains complex due to the incompletely understood mechanisms of contrast formation of cryogenic, unstained biological specimens. While the contrast is suggested to arise from differential surface potential and local charging, additional factors may also contribute (Schertel et al., 2013; Vidavsky et al., 2016). With the growing attention on cryo-FIB-ET, the 3D FIB-SEM technique is expected to become more widely accessible, as it can be performed using the same instrumentation available in many laboratories for lamella production. Widespread application will likely require theoretical developments in understanding image formation, and in the development of streamlined strategies for data analysis. We hope further software and hardware advancements will address the current challenges, for example by reducing the ion beam size to allow finer slicing of the sample, as well as improved SEM detectors that can decrease the dwell time and allow faster imaging.

In the same vein as FIB-SEM imaging, another alternative method to investigate whole cells or tissues in 3D is cryo-scanning transmission electron microscopy (STEM), which uses a focused electron beam probe rather than flood beam used in TEM applications (Jones & Leonard, 1978; Kellenberger et al., 1986). Cryo-STEM allows scanning over the sample in a tiled manner using multiple detectors that collect information for both transmitted and scattered electrons (Elbaum et al., 2021; Wolf & Elbaum, 2019). While samples up to 2 μm in thickness can potentially be imaged using cryo-STEM, in practice to obtain data with a good contrast and a reasonable pixel size, the effective specimen thickness is usually less than 1 μm (Kirchweger et al., 2023; Wolf et al., 2014). Cryo-STEM has been successfully utilised to visualise whole cells (Wolf et al., 2014), organelles containing granular calcium structures (Kirchweger et al., 2023; Wolf et al., 2017), single particle reconstructions at sub-nanometre resolutions of purified proteins and virus particles (Lazić et al., 2022), as well as metal ion composition and localisation in purified proteins (Elad et al., 2017). Cryo-STEM is therefore a complementary technique for cellular imaging, providing another arrow in the quiver of the *in situ* structural cell biologist.

Another cryo-tomography technique which has been recently used to investigate large cells and tissues, albeit at lower resolution, is cryo-soft X-ray tomography (cryo-SXT), which can provide information through specimens that are several microns thick (Larabell & Le Gros, 2004; Weiß et al., 2000). In cryo-SXT, contrast is naturally generated by the difference in the K-shell absorption of soft X-rays between carbon (or nitrogen) and oxygen in wavelengths ranging between 2.34–4.4 nm (Larabell & Nugent, 2010). Imaging in this spectral range, also termed the 'water window', causes organic material, which is abundantly present in cells and organelles to absorb the X-rays, while water and other oxygen rich compounds are effectively transparent (Carzaniga et al., 2014; Larabell & Le Gros, 2004). Cryo-SXT offers not only a large depth of field, which can reach 10–15 μm (Carzaniga et al., 2014; J. Guo & Larabell, 2019; Uchida et al., 2009), but also a large field of view together with fast data acquisition times, where unstained and unmodified cells nearly 50 μm in length can be imaged in 20 minutes with a resolution of about 50 nm (Larabell & Nugent, 2010; Uchida et al., 2009). This is much faster when compared to 3D FIB-SEM or cryo-STEM which take several hours or days to collect a dataset of a similar scale. Recent advancements in cryo-SXT include improvement of data collection schemes to increase the depth of field (Otón et al., 2017); however, the most substantial is the transition from synchrotron-based microscopes into compact, standalone machines which can be operated in a typical laboratory (Fahy et al., 2021, 2024), which is expected to make this method available to a wider community.

Conclusions and outlook

In conclusion, we have reviewed recent advances pertaining to sample preparation, thinning strategies and cryo-ET data collection schemes, which are currently being used to investigate multicellular specimens and tissues *in situ*. From the sample preparation perspective, there is currently no method that can allow a reliable vitrification of specimens thicker than 100–200 μm, meaning that most tissues are currently not directly amenable for imaging by cryo-ET, and innovation in this aspect is urgently needed. This could be achieved by repurposing HPF to accommodate thicker specimens, or by devising alternative techniques for sample preparation. While metal ion beam sources have been used extensively in materials sciences as well as for biological cryo-FIB sample thinning, they are still limited by a low rate of material removal and hence prevent easy access to thicker tissue samples. Investigating different focused ion beams is required to allow faster and more reliable milling, ideally with the potential to reduce the damage the sample undergoes during thinning. As automation and increased

https://doi.org/10.1017/S0033583525000010 Published online by Cambridge University Press

throughput are introduced to the FIB milling process, cryo-ET data collection must also improve to allow tomogram acquisition from multiple lamellae across multiple grids. Beam-shift collection schemes could greatly increase the rate of data collection without compromising data quality, but there is room for improvement in making this available for all sorts of applications. To tackle the densely packed cellular environment, and increase the overall contrast of tomograms, the laser phase plate is expected to push the limits of macromolecular identification in tomograms. These and other approaches might help generate higher-resolution tomograms, where sub-nanometre-level details could be resolved and inferred directly from the reconstructed tomogram, without the need for subtomogram averaging. We envision that future cryo-EM instruments will include a combination of multimodal components such as cryo-FIB-SEM, light microscopy objectives and mass spectrometers, that will complement TEM data acquisition, with cryo-ET as the central method of choice linking information from these diverse sources together to help uncover new biological mechanisms.

Acknowledgements. This work was supported by the Medical Research Council, as part of United Kingdom Research and Innovation (also known as UK Research and Innovation) [Programme MC_UP_1201/31 to T.A.M.B.]. T.A.M.B. would like to thank EPSRC (Grant EP/V026623/1), the European Molecular Biology Organization, the Wellcome Trust (Grant 225317/Z/22/Z), the Leverhulme Trust, and the Lister Institute for Preventative Medicine for support. I.C. was supported by an EMBO Long-Term Fellowship (ALTF 92-2022).

Competing interest. The authors declare no competing interests.

References

Al-Amoudi A, Norlen LPO and Dubochet J (2004) Cryo-electron microscopy of vitreous sections of native biological cells and tissues. *Journal of Structural Biology* **148**(1), 131–135. https://doi.org/10.1016/J.JSB.2004.03.010

Al-Amoudi A, Studer D and Dubochet J (2005) Cutting artefacts and cutting process in vitreous sections for cryo-electron microscopy. *Journal of Structural Biology* **150**(1), 109–121. https://doi.org/10.1016/J.JSB.2005.01.003

Allegretti M, Zimmerli CE, Rantos V, Wilfling F, Ronchi P, Fung HKH, Lee CW, Hagen W, Turoňová B, Karius K, Börmel M, Zhang X, Müller CW, Schwab Y, Mahamid J, Pfander B, Kosinski J and Beck M (2020) In-cell architecture of the nuclear pore and snapshots of its turnover. *Nature* **586**(7831), 796–800. https://doi.org/10.1038/s41586-020-2670-5

Axelrod JJ, Petrov PN, Zhang JT, Remis J, Buijsse B, Glaeser RM and Müller H (2023) Overcoming resolution loss due to thermal magnetic field fluctuations from phase plates in transmission electron microscopy. *Ultramicroscopy* **249**, 113730. https://doi.org/10.1016/J.ULTRAMIC.2023.113730

Axelrod JJ, Petrov PN, Zhang JT, Sandhaus S, Remis J, Glaeser RM and Müller H (2023) Overcoming resolution loss in laser phase plate cryo-electron microscopy. *Microscopy and Microanalysis* **29**(Supplement_1), 1017–1017. https://doi.org/10.1093/MICMIC/OZAD067.513

Bäuerlein FJB, Renner M, Chami DEl, Lehnart SE, Pastor-Pareja JC and Fernández-Busnadiego R (2023) Cryo-electron tomography of large biological specimens vitrified by plunge freezing. *BioRxiv*, 2021.04.14.437159. https://doi.org/10.1101/2021.04.14.437159

Baumeister W (2005) From proteomic inventory to architecture. *FEBS Letters* **579**(4), 933–937. https://doi.org/10.1016/J.FEBSLET.2004.10.102

Baumeister W, Grimm R and Walz J (1999) Electron tomography of molecules and cells. *Trends in Cell Biology* **9**(2), 81–85. https://doi.org/10.1016/S0962-8924(98)01423-8

Beck M and Baumeister W (2016) Cryo-electron tomography: Can it reveal the molecular sociology of cells in atomic detail? *Trends in Cell Biology* **26**(11), 825–837. https://doi.org/10.1016/J.TCB.2016.08.006

Berger C, Dumoux M, Glen T, Yee NBy., Mitchels JM, Patáková Z, Darrow MC, Naismith JH and Grange M (2023) Plasma FIB milling for the determination of structures in situ. *Nature Communications* **14**(1), 1–12. https://doi.org/10.1038/s41467-023-36372-9

Berger C, Premaraj N, Ravelli RBG, Knoops K, López-Iglesias C and Peters PJ (2023) Cryo-electron tomography on focused ion beam lamellae transforms structural cell biology. *Nature Methods* **20**(4), 499–511. https://doi.org/10.1038/s41592-023-01783-5

Berger C, Watson H, Naismith J, Dumoux M and Grange M (2024) Xenon plasma focused ion beam lamella fabrication on high-pressure frozen specimens for structural cell biology. *BioRxiv*, 2024.06.20.599830. https://doi.org/10.1101/2024.06.20.599830

Bharat TAM, Hoffmann PC and Kukulski W (2018) Correlative microscopy of vitreous sections provides insights into BAR-domain organization in situ. *Structure* **26**(6), 879–886.e3. https://doi.org/10.1016/J.STR.2018.03.015

Bharat T.AM, Russo CJ, Löwe J, Passmore LA and Scheres SHW (2015) Advances in single-particle electron cryomicroscopy structure determination applied to sub-tomogram averaging. *Structure* **23**(9), 1743. https://doi.org/10.1016/J.STR.2015.06.026

Bock LV and Grubmüller H (2022) Effects of cryo-EM cooling on structural ensembles. *Nature Communications* **13**(1), 1–13. https://doi.org/10.1038/s41467-022-29332-2

Böhning J and Bharat TAM (2021) Towards high-throughput in situ structural biology using electron cryotomography. *Progress in Biophysics and Molecular Biology* **160**, 97–103. https://doi.org/10.1016/J.PBIOMOLBIO.2020.05.010

Bouvette J, Liu HF, Du X, Zhou Y, Sikkema AP, da Fonseca Rezende e Mello J, Klemm BP, Huang R, Schaaper RM, Borgnia MJ and Bartesaghi A (2021) Beam image-shift accelerated data acquisition for near-atomic resolution single-particle cryo-electron tomography. *Nature Communications* **12**(1), 1–11. https://doi.org/10.1038/s41467-021-22251-8

Briggs JAG (2013) Structural biology in situ--The potential of subtomogram averaging. *Current Opinion in Structural Biology* **23**(2), 261–267. https://doi.org/10.1016/J.SBI.2013.02.003

Brown HG, Smith D, Wardle BC and Hanssen E (2024) Square condenser apertures for square cameras in low-dose transmission electron microscopy. *Nature Methods* **21**(4), 566–568. https://doi.org/10.1038/s41592-024-02206-9

Buchholz TO, Jordan M, Pigino G and Jug F (2018) Cryo-CARE: Content-aware image restoration for cryo-transmission electron microscopy data. In *Proceedings - International Symposium on Biomedical Imaging*, 2019 April, 502–506. https://doi.org/10.1109/ISBI.2019.8759519

Burnett TL, Kelley R, Winiarski B, Contreras L, Daly M, Gholinia A, Burke MG and Withers PJ (2016) Large volume serial section tomography by Xe plasma FIB dual beam microscopy. *Ultramicroscopy* **161**, 119–129. https://doi.org/10.1016/J.ULTRAMIC.2015.11.001

Burt A, Toader B, Warshamanage R, von Kügelgen A, Pyle E, Zivanov J, Kimanius D, Bharat TAM and Scheres SHW (2024) An image processing pipeline for electron cryo-tomography in RELION-5. *FEBS Open Bio*. https://doi.org/10.1002/2211-5463.13873

Campbell SL, Schwartz O, Axelrod JJ, Turnbaugh C, Glaeser RM and Müller H (2018) A laser-based phase plate for phase contrast transmission electron microscopy. *Frontiers in Optics/Laser Science, Part F114-FIO 2018*, FW7B.5. https://doi.org/10.1364/FIO.2018.FW7B.5

Capua-Shenkar J, Varsano N, Itzhak NR, Kaplan-Ashiri I, Rechav K, Jin X, Niimi M, Fan J, Kruth HS and Addadi L (2022) Examining atherosclerotic lesions in three dimensions at the nanometer scale with cryo-FIB-SEM. *Proceedings of the National Academy of Sciences of the United States of America* **119**(34), e2205475119. https://doi.org/10.1073/PNAS.2205475119

Carzaniga R, Domart MC, Collinson LM and Duke E (2014) Cryo-soft X-ray tomography: A journey into the world of the native-state cell. *Protoplasma* **251**(2), 449–458. https://doi.org/10.1007/S00709-013-0583-Y

Chaillet ML, Roet S, Veltkamp RC and Förster F (2024) Pytom-match-pick: A Tophat-transform constraint for automated classification in template matching. *BioRxiv*, 2024.09.17.613497. https://doi.org/10.1101/2024.09.17.613497

Chang IY, Rahman M, Harned A, Cohen-Fix O and Narayan K (2021) Cryo-fluorescence microscopy of high-pressure frozen *C. elegans* enables correlative FIB-SEM imaging of targeted embryonic stages in the intact worm. *Methods in Cell Biology* **162**, 223. https://doi.org/10.1016/BS.MCB.2020.09.009

Chang Y, Lu W, Guénolé J, Stephenson LT, Szczpaniak A, Kontis P, Ackerman AK, Dear FF, Mouton I, Zhong X, Zhang S, Dye D, Liebscher CH, Ponge D, Korte-Kerzel S, Raabe D and Gault B (2019) Ti and its alloys as

examples of cryogenic focused ion beam milling of environmentally-sensitive materials. *Nature Communications* **10**(1), 1–10. https://doi.org/10.1038/s41467-019-08752-7

Chen M, Bell JM, Shi X, Sun SY, Wang Z and Ludtke SJ (2019) A complete data processing workflow for cryo-ET and subtomogram averaging. *Nature Methods* **16**(11), 1161–1168. https://doi.org/10.1038/s41592-019-0591-8

Chen S, Basiashvili T, Hutchings J, Murillo MS, Suarez AV, Louro JA, Leschziner AE and Villa E (2024) Cryo-electron tomography reveals the microtubule-bound form of inactive LRRK2. *ELife* **13**. https://doi.org/10.7554/ELIFE.100799.1

Chen Z, Shiozaki M, Haas KM, Skinner WM, Zhao S, Guo C, Polacco BJ, Yu Z, Krogan NJ, Lishko PV, Kaake RM, Vale RD and Agard DA (2023) De novo protein identification in mammalian sperm using in situ cryoelectron tomography and AlphaFold2 docking. *Cell* **186**(23), 5041–5053.e19. https://doi.org/10.1016/J.CELL.2023.09.017

Chreifi G, Chen S and Jensen GJ (2021) Rapid tilt-series method for cryo-electron tomography: Characterizing stage behavior during FISE acquisition. *Journal of Structural Biology* **213**(2), 107716. https://doi.org/10.1016/J.JSB.2021.107716

Chreifi G, Chen S, Metskas LA, Kaplan M and Jensen GJ (2019) Rapid tilt-series acquisition for electron cryotomography. *Journal of Structural Biology* **205**(2), 163–169. https://doi.org/10.1016/J.JSB.2018.12.008

Chua EYD, Alink LM, Kopylov M, Johnston JD, Eisenstein F and de Marco A (2024) Square beams for optimal tiling in transmission electron microscopy. *Nature Methods* **21**(4), 562–565. https://doi.org/10.1038/s41592-023-02161-x

Cleeve P, Caggiano MP, Dierickx D, Whisstock J and de Marco A (2023) Automation in Cryo-FIB preparation, from cellular to tissue structural biology. *Microscopy and Microanalysis* **29**(29 Suppl 1), 1956. https://doi.org/10.1093/MICMIC/OZAD067.1013

Creekmore BC, Kixmoeller K, Black BE, Lee EB and Chang YW (2024) Ultrastructure of human brain tissue vitrified from autopsy revealed by cryo-ET with cryo-plasma FIB milling. *Nature Communications* **15**(1), 1–12. https://doi.org/10.1038/s41467-024-47066-1

Cruz-León S, Majtner T, Hoffmann PC, Kreysing JP, Kehl S, Tuijtel MW, Schaefer SL, Geißler K, Beck M, Turoňová B and Hummer G (2024) High-confidence 3D template matching for cryo-electron tomography. *Nature Communications* **15**(1), 1–14. https://doi.org/10.1038/s41467-024-47839-8

Dahl R and Staehelin LA (1989) Highpressure freezing for the preservation of biological structure: Theory and practice. *Journal of Electron Microscopy Technique* **13**(3), 165–174. https://doi.org/10.1002/JEMT.1060130305

Dandey VP, Budell WC, Wei H, Bobe D, Maruthi K, Kopylov, M, Eng ET, Kahn PA, Hinshaw JE, Kundu N, Nimigean CM, Fan C, Sukomon N, Darst SA, Saecker RM, Chen J, Malone B, Potter CS and Carragher B (2020) Time-resolved cryo-EM using Spotiton. *Nature Methods* **17**(9), 897–900. https://doi.org/10.1038/s41592-020-0925-6

De Rosier DJ and Klug A (1968) Reconstruction of three dimensional structures from electron micrographs. *Nature* **217**(5124), 130–134. https://doi.org/10.1038/217130a0

de Teresa-Trueba I, Goetz SK, Mattausch A, Stojanovska F, Zimmerli CE, Toro-Nahuelpan M, Cheng DWC, Tollervey F, Pape C, Beck M, Diz-Muñoz A, Kreshuk A, Mahamid J and Zaugg JB (2023) Convolutional networks for supervised mining of molecular patterns within cellular context. *Nature Methods* **20**(2), 284–294. https://doi.org/10.1038/s41592-022-01746-2

Denk W and Horstmann H (2004) Serial block-face scanning electron microscopy to reconstruct three-dimensional tissue nanostructure. *PLoS Biology* **2**(11) https://doi.org/10.1371/journal.pbio.0020329

D'Imprima E, Garcia Montero M, Gawrzak S, Ronchi P, Zagoriy I, Schwab Y, Jechlinger M and Mahamid J (2023) Light and electron microscopy continuum-resolution imaging of 3D cell cultures. *Developmental Cell* **58**(7), 616–632.e6. https://doi.org/10.1016/J.DEVCEL.2023.03.001

Du DX and Fitzpatrick AWP (2023) Design of an ultrafast pulsed ponderomotive phase plate for cryo-electron tomography. *Cell Reports Methods* **3**(1), 100387. https://doi.org/10.1016/J.CRMETH.2022.100387

Dubochet J, Adrian M, Chang J-J, Homo J-C, Lepault J, McDowall AW and Schultz P (1988) Cryo-electron microscopy of vitrified specimens. *Quarterly Reviews of Biophysics* **21**(2), 129–228. https://doi.org/10.1017/S0033583500004297

Dubochet J and McDowall AW (1981) Vitrification of pure water for electron microscopy. *Journal of Microscopy* **124**(3), 3–4. https://doi.org/10.1111/J.1365-2818.1981.TB02483.X

Dumoux M, Glen T, Smith JL, Ho EM, Perdigão LM, Pennington A, Klumpe S, Yee NB, Farmer DA, Lai PY, Bowles W, Kelley R, Plitzko JM, Wu L, Basham M, Clare DK, Siebert CA, Darrow MC, Naismith JH and Grange M (2023) Cryo-plasma FIB/SEM volume imaging of biological specimens. *ELife* **12**. https://doi.org/10.7554/ELIFE.83623

Eder K, Bhatia V, Qu J, Van Leer B, Dutka M and Cairney JM (2021) A multi-ion plasma FIB study: Determining ion implantation depths of Xe, N, O and Ar in tungsten via atom probe tomography. *Ultramicroscopy* **228**, 113334. https://doi.org/10.1016/J.ULTRAMIC.2021.113334

Eisenstein F, Danev R and Pilhofer M (2019) Improved applicability and robustness of fast cryo-electron tomography data acquisition. *Journal of Structural Biology* **208**(2), 107–114. https://doi.org/10.1016/J.JSB.2019.08.006

Eisenstein F, Fukuda Y and Danev R (2023) Smart parallel automated cryo electron tomography. *BioRxiv*, 2023.12.14.571776. https://doi.org/10.1101/2023.12.14.571776

Eisenstein F, Yanagisawa H, Kashihara H, Kikkawa M, Tsukita S and Danev R (2022) Parallel cryo electron tomography on in situ lamellae. *Nature Methods* **20**(1), 131–138. https://doi.org/10.1038/s41592-022-01690-1

Elad N, Bellapadrona G, Houben L, Sagi I and Elbaum M (2017) Detection of isolated protein-bound metal ions by single-particle cryo-STEM. *Proceedings of the National Academy of Sciences of the United States of America* **114**(42), 11139–11144. https://doi.org/10.1073/pnas.1708609114

Elbaum M (2018) Expanding horizons of cryo-tomography to larger volumes. *Current Opinion in Microbiology* **43**, 155–161. https://doi.org/10.1016/J.MIB.2018.01.001

Elbaum M, Seifer S, Houben L, Wolf SG and Rez P (2021) Toward compositional contrast by cryo-STEM. *Accounts of Chemical Research* **54**(19), 3621–3631. https://doi.org/10.1021/ACS.ACCOUNTS.1C00279

Eltsov M, Grewe D, Lemercier N, Frangakis A, Livolant F and Leforestier A (2018) Nucleosome conformational variability in solution and in interphase nuclei evidenced by cryo-electron microscopy of vitreous sections. *Nucleic Acids Research* **46**(17), 9189–9200. https://doi.org/10.1093/NAR/GKY670

Esser TK, Böhning J, Önür A, Chinthapalli DK, Eriksson L, Grabarics M, Fremdling P, Konijnenberg A, Makarov A, Botman A, Peter C, Benesch JLP., Robinson CV, Gault J, Baker L, Bharat TAM. and Rauschenbach S (2024) Cryo-EM of soft-landed β-galactosidase: Gas-phase and native structures are remarkably similar. *Science Advances* **10**(7), 4628. https://doi.org/10.1126/SCIADV.ADL4628

Fahy K, Kapishnikov S, Donnellan M, McEnroe T, O'Reilly F, Fyans W and Sheridan P (2024) Laboratory based correlative cryo-soft X-ray tomography and cryo-fluorescence microscopy. *Methods in Cell Biology* **187**, 293–320. https://doi.org/10.1016/BS.MCB.2024.02.033

Fahy K, Weinhardt V, Vihinen-Ranta M, Fletcher N, Skoko D, Pereiro E, Gastaminza P, Bartenschlager R, Scholz D, Ekman A and McEnroe T (2021) Compact cell imaging device (CoCID) provides insights into the cellular origins of viral infections. *Journal of Physics: Photonics* **3**(3), 031002. https://doi.org/10.1088/2515-7647/ABFC5A

Fedry J, Silva J, Vanevic M, Fronik S, Mechulam Y, Schmitt E, des Georges A, Faller WJ and Förster F (2024) Visualization of translation reorganization upon persistent ribosome collision stress in mammalian cells. *Molecular Cell* **84**(6), 1078–1089.e4. https://doi.org/10.1016/J.MOLCEL.2024.01.015

Förster F, Medalia O, Zauberman N, Baumeister W and Fass D (2005) Retrovirus envelope protein complex structure in situ studied by cryo-electron tomography. *Proceedings of the National Academy of Sciences of the United States of America* **102**(13), 4729–4734. https://doi.org/10.1073/PNAS.0409178102

Frank J (1995) Approaches to large-scale structures. *Current Opinion in Structural Biology* **5**(2), 194–201. https://doi.org/10.1016/0959-440X(95)80075-1

Fuest M, Schaffer M, Nocera GM, Galilea-Kleinsteuber RI, Messling JE, Heymann M, Plitzko JM and Burg TP (2019) In situ microfluidic cryofixation for cryo focused ion beam milling and cryo electron tomography. *Scientific Reports* **9**(1), 1–10. https://doi.org/10.1038/s41598-019-55413-2

Gan L and Jensen GJ (2012) Electron tomography of cells. *Quarterly Reviews of Biophysics* **45**(1), 27–56. https://doi.org/10.1017/S0033583511000102

https://doi.org/10.1017/S0033583525000010 Published online by Cambridge University Press

Gemmer M, Chaillet ML, van Loenhout J, Cuevas Arenas R, Vismpas D, Gröllers-Mulderij M, Koh FA, Albanese P, Scheltema RA, Howes SC, Kotecha A, Fedry J and Förster F (2023) Visualization of translation and protein biogenesis at the ER membrane. *Nature* **614**(7946), 160–167. https://doi.org/10.1038/s41586-022-05638-5

Gilbert MAG, Fatima N, Jenkins J, O'Sullivan TJ, Schertel A, Halfon Y, Wilkinson M, Morrema THJ, Geibel M, Read RJ, Ranson NA, Radford SE, Hoozemans JJM and Frank RAW (2024) CryoET of β-amyloid and tau within postmortem Alzheimer's disease brain. *Nature* **631**(8022), 913–919. https://doi.org/10.1038/s41586-024-07680-x

Gorelick S and De Marco A (2018) Fabrication of glass microlenses using focused Xe beam. *Optics Express* **26**(10), 13647–13655. https://doi.org/10.1364/OE.26.013647

Guo J and Larabell CA (2019) Soft X-ray tomography: Virtual sculptures from cell cultures. *Current Opinion in Structural Biology* **58**, 324–332. https://doi.org/10.1016/J.SBI.2019.06.012

Guo Q, Lehmer C, Martínez-Sánchez A, Rudack T, Beck F, Hartmann H, Pérez-Berlanga M, Frottin F, Hipp MS, Hartl FU, Edbauer D, Baumeister W and Fernández-Busnadiego R (2018) In situ structure of neuronal C9orf72 poly-GA aggregates reveals proteasome recruitment. *Cell* **172**(4), 696–705.e12. https://doi.org/10.1016/J.CELL.2017.12.030

Harapin J, Börmel M, Sapra KT, Brunner D, Kaech A and Medalia O (2015) Structural analysis of multicellular organisms with cryo-electron tomography. *Nature Methods* **12**(7), 634–636. https://doi.org/10.1038/nmeth.3401

Held RG, Liang J and Brunger AT (2024) Nanoscale architecture of synaptic vesicles and scaffolding complexes revealed by cryo-electron tomography. *Proceedings of the National Academy of Sciences of the United States of America* **121**(27), e2403136121. https://doi.org/10.1073/PNAS.2403136121

Henderson R (1992) Image contrast in high-resolution electron microscopy of biological macromolecules: TMV in ice. *Ultramicroscopy* **46**(1–4), 1–18. https://doi.org/10.1016/0304-3991(92)90003-3

Henderson R (2004) Realizing the potential of electron cryo-microscopy. *Quarterly Reviews of Biophysics* **37**(1), 3–13. https://doi.org/10.1017/S0033583504003920

Heymann JAW, Hayles M, Gestmann I, Giannuzzi LA, Lich B and Subramaniam S (2006) Site-specific 3D imaging of cells and tissues with a dual beam microscope. *Journal of Structural Biology* **155**(1), 63–73. https://doi.org/10.1016/J.JSB.2006.03.006

Himes BA and Zhang P (2018) emClarity: Software for high-resolution cryo-electron tomography and subtomogram averaging. *Nature Methods* **15**(11), 955–961. https://doi.org/10.1038/s41592-018-0167-z

Hoffmann PC, Kreysing JP, Khusainov I, Tuijtel MW, Welsch S and Beck M (2022) Structures of the eukaryotic ribosome and its translational states in situ. *Nature Communications* **13**(1), 1–9. https://doi.org/10.1038/s41467-022-34997-w

Hoppe W (1970) Principles of electron structure research at atomic resolution using conventional electron microscopes for the measurement of amplitudes and phases. *Acta Cryst* **26**, 414.

Hoppe W (1974) Towards three-dimensional "electron microscopy" at atomic resolution. *Die Naturwissenschaften* **61**(6), 239–249. https://doi.org/10.1007/BF00595655

Hutchings J, Stancheva V, Miller EA and Zanetti G (2018) Subtomogram averaging of COPII assemblies reveals how coat organization dictates membrane shape. *Nature Communications* **9**(1) https://doi.org/10.1038/S41467-018-06577-4

Hutchings J and Zanetti G (2018) Fine details in complex environments: The power of cryo-electron tomography. *Biochemical Society Transactions* **46**(4), 807. https://doi.org/10.1042/BST20170351

Iulianella A (2017) Cutting thick sections using a vibratome. *Cold Spring Harbor Protocols* **2017**(6), 505–508. https://doi.org/10.1101/PDB.PROT094011

Jentoft IMA, Bäuerlein FJB, Welp LM, Cooper BH, Petrovic A, So C, Penir SM, Politi AZ, Horokhovskyi Y, Takala I, Eckel H, Moltrecht R, Lénárt P, Cavazza T, Liepe J, Brose N, Urlaub H, Fernández-Busnadiego R and Schuh M (2023) Mammalian oocytes store proteins for the early embryo on cytoplasmic lattices. *Cell* **186**(24), 5308–5327.e25. https://doi.org/10.1016/J.CELL.2023.10.003

Jones AV and Leonard KR (1978) Scanning transmission electron microscopy of unstained biological sections. *Nature* **271**(5646), 659–660. https://doi.org/10.1038/271659a0

Jumper J, Evans R, Pritzel A, Green T, Figurnov M, Ronneberger O, Tunyasuvunakool K, Bates R, Žídek A, Potapenko A, Bridgland A, Meyer C, Kohl SAA, Ballard AJ, Cowie A, Romera-Paredes B, Nikolov S, Jain R, Adler J, … Hassabis D (2021) Highly accurate protein structure prediction with AlphaFold. *Nature* **596**(7873), 583–589. https://doi.org/10.1038/s41586-021-03819-2

Kellenberger E, Carlemalm E, Villiger W, Wurtz M, Mory C and Colliex C (1986) Z-contrast in biology: A comparison with other imaging modes. *Annals of the New York Academy of Sciences* **483**(1), 202–228. https://doi.org/10.1111/J.1749-6632.1986.TB34522.X

Kelley K, Raczkowski AM, Klykov O, Jaroenlak P, Bobe D, Kopylov M, Eng ET, Bhabha G, Potter CS, Carragher B and Noble AJ (2022) Waffle method: A general and flexible approach for improving throughput in FIB-milling. *Nature Communications* **13**(1), 1–13. https://doi.org/10.1038/s41467-022-29501-3

Kirchweger P, Mullick D, Wolf SG and Elbaum M (2023) Visualization of organelles in situ by cryo-STEM tomography. *Journal of Visualized Experiments (JoVE)* **2023**(196), e65052. https://doi.org/10.3791/65052

Klumpe S, Fung HKH, Goetz SK, Zagoriy I, Hampoelz B, Zhang X, Erdmann PS, Baumbach J, Müller CW, Beck M, Plitzko JM and Mahamid J (2021) A modular platform for automated cryo-FIB Workflows. *ELife* **10**. https://doi.org/10.7554/ELIFE.70506

Klumpe S, Kuba J, Schioetz OH, Erdmann PS, Rigort A and Plitzko JM (2022) Recent advances in gas injection system-free cryo-FIB lift-out transfer for cryo-electron tomography of multicellular organisms and tissues. *Microscopy Today* **30**(1), 42–47. https://doi.org/10.1017/S1551929521001528

Klumpe S, Schioetz OH, Kaiser C, Luchner M, Brenner J and Plitzko JM (2023) Developments in cryo-FIB sample preparation: Targeting in cryo-lift-out preparation of tissues and machine learning models for fully automated on-grid lamella preparation. *Microscopy and Microanalysis* **29**(Supplement_1), 511–513. https://doi.org/10.1093/MICMIC/OZAD067.243

Koeck PJB and Karshikoff A (2015) Limitations of the linear and the projection approximations in three-dimensional transmission electron microscopy of fully hydrated proteins. *Journal of Microscopy* **259**(3), 197–209. https://doi.org/10.1111/JMI.12253

Kravčenko U, Ruwolt M, Kroll J, Yushkevich A, Zenkner M, Ruta J, Lotfy R, Wanker EE, Rosenmund C, Liu F and Kudryashev M (2024) Molecular architecture of synaptic vesicles. *Proceedings of the National Academy of Sciences of the United States of America* **121**(49), e2407375121. https://doi.org/10.1073/PNAS.2407375121

Kremer JR, Mastronarde DN and McIntosh JR (1996) Computer visualization of three-dimensional image data using IMOD. *Journal of Structural Biology* **116**(1), 71–76. https://doi.org/10.1006/JSBI.1996.0013

Kuba J, Mitchels J, Hovorka M, Erdmann P, Berka L, Kirmse R, König J, De Bock J, Goetze B and Rigort A (2021) Advanced cryo-tomography workflow developments – correlative microscopy, milling automation and cryo-lift-out. *Journal of Microscopy* **281**(2), 112–124. https://doi.org/10.1111/JMI.12939

Kühlbrandt W (2014) The resolution revolution. *Science* **343**(6178), 1443–1444. https://doi.org/10.1126/science.1251652

Lai WC, Lin CY, Chang WT, Li PC, Fu TY, Chang CS, Tsong TT and Hwang IS (2017) Xenon gas field ion source from a single-atom tip. *Nanotechnology* **28**(25), 255301. https://doi.org/10.1088/1361-6528/AA6ED3

Lam V and Villa E (2021) Practical approaches for cryo-FIB milling and applications for cellular cryo-electron tomography. *Methods in Molecular Biology* **2215**, 49–82. https://doi.org/10.1007/978-1-0716-0966-8_3

Larabell CA and Le Gros MA (2004) X-ray tomography generates 3-D reconstructions of the yeast, *Saccharomyces cerevisiae*, at 60-nm resolution. *Molecular Biology of the Cell* **15**(3), 957. https://doi.org/10.1091/MBC.E03-07-0522

Larabell CA and Nugent KA (2010) Imaging cellular architecture with X-rays. *Current Opinion in Structural Biology* **20**(5), 623. https://doi.org/10.1016/J.SBI.2010.08.008

Lazić I, Wirix M, Leidl ML, de Haas F, Mann D, Beckers M, Pechnikova EV, Müller-Caspary K, Egoavil R, Bosch EGT and Sachse C (2022) Single-particle cryo-EM structures from iDPC–STEM at near-atomic resolution.

Nature Methods **19**(9), 1126–1136. https://doi.org/10.1038/s41592-022-01586-0

Leistner C, Wilkinson M, Burgess A, Lovatt M, Goodbody S, Xu Y, Deuchars S, Radford SE, Ranson NA and Frank RAW (2023) The in-tissue molecular architecture of β-amyloid pathology in the mammalian brain. *Nature Communications* **14**(1), 1–12. https://doi.org/10.1038/s41467-023-38495-5

Leung MR, Zeng J, Wang X, Roelofs MC, Huang W, Zenezini Chiozzi R, Hevler JF, Heck AJR, Dutcher, SK, Brown A, Zhang R and Zeev-Ben-Mordehai T (2023) Structural specializations of the sperm tail. *Cell* **186**(13), 2880–2896.e17. https://doi.org/10.1016/j.cell.2023.05.026

Lindell AE, Grießhammer A, Michaelis L, Papagiannidis D, Ochner H, Kamrad S, Guan R, Blasche S, Ventimiglia L, Ramachandran B, Ozgur H, Zelezniak A, Beristain-Covarrubias N, Yam-Puc JC, Roux I, Barron LP, Richardson AK, Martin MG, Benes V, … Patil KR (2024) Extensive PFAS accumulation by human gut bacteria. *BioRxiv*, 2024.09.17.613493. https://doi.org/10.1101/2024.09.17.613493

Liu HF, Zhou Y, Huang Q, Piland J, Jin W, Mandel J, Du X, Martin J and Bartesaghi A (2023) nextPYP: A comprehensive and scalable platform for characterizing protein variability in situ using single-particle cryo-electron tomography. *Nature Methods* **20**(12), 1909–1919. https://doi.org/10.1038/s41592-023-02045-0

Liu YT, Zhang H, Wang H, Tao CL, Bi GQ and Zhou ZH (2022) Isotropic reconstruction for electron tomography with deep learning. *Nature Communications* **13**(1), 1–17. https://doi.org/10.1038/s41467-022-33957-8

Lucas BA and Grigorieff N (2023) Quantification of gallium cryo-FIB milling damage in biological lamellae. *Proceedings of the National Academy of Sciences of the United States of America* **120**(23), e2301852120. https://doi.org/10.1073/PNAS.2301852120

Lucas BA, Himes BA and Grigorieff N (2023) Baited reconstruction with 2D template matching for high-resolution structure determination in vitro and in vivo without template bias. *ELife*, **12**. https://doi.org/10.7554/ELIFE.90486.2

Lučić V, Rigort A and Baumeister W (2013) Cryo-electron tomography: The challenge of doing structural biology in situ. *Journal of Cell Biology* **202**(3), 407–419. https://doi.org/10.1083/JCB.201304193

Ma OX, Chong WG, Lee JKE, Cai S, Siebert CA, Howe A, Zhang P, Shi J, Surana U and Gan L (2022) Cryo-ET detects bundled triple helices but not ladders in meiotic budding yeast. *PLOS ONE* **17**(4), e0266035. https://doi.org/10.1371/JOURNAL.PONE.0266035

Mahamid J, Pfeffer S, Schaffer M, Villa E, Danev R, Cuellar LK, Förster F, Hyman AA, Plitzko JM and Baumeister W (2016) Visualizing the molecular sociology at the HeLa cell nuclear periphery. *Science* **351**(6276), 969–972. https://doi.org/10.1126/SCIENCE.AAD8857

Mahamid J, Schampers R, Persoon H, Hyman AA, Baumeister W and Plitzko JM (2015) A focused ion beam milling and lift-out approach for site-specific preparation of frozen-hydrated lamellas from multicellular organisms. *Journal of Structural Biology* **192**(2), 262–269. https://doi.org/10.1016/J.JSB.2015.07.012

Marko M, Hsieh C, Moberlychan W, Mannella CA and Frank J (2006) Focused ion beam milling of vitreous water: Prospects for an alternative to cryo-ultramicrotomy of frozen-hydrated biological samples. *Journal of Microscopy* **222**(1), 42–47. https://doi.org/10.1111/J.1365-2818.2006.01567.X

Marko M, Hsieh C, Schalek R, Frank J and Mannella C (2007) Focused-ion-beam thinning of frozen-hydrated biological specimens for cryo-electron microscopy. *Nature Methods* **4**(3), 215–217. https://doi.org/10.1038/nmeth1014

Mastronarde DN (2005) Automated electron microscope tomography using robust prediction of specimen movements. *Journal of Structural Biology* **152**(1), 36–51. https://doi.org/10.1016/J.JSB.2005.07.007

Matsui A, Spangler CJ, Elferich J, Shiozaki M, Jean N, Zhao X, Qin M, Zhong H, Yu Z and Gouaux E (2024) Cryo-electron tomographic investigation of native hippocampal glutamatergic synapses. *ELife* **13**. https://doi.org/10.7554/ELIFE.98458.2

Mattei S, Glass B, Hagen WJH, Kräusslich HG and Briggs JAG (2016) The structure and flexibility of conical HIV-1 capsids determined within intact virions. *Science* **354**(6318), 1434–1437. https://doi.org/10.1126/SCIENCE.AAH4972

McCafferty CL, Klumpe S, Amaro RE, Kukulski W, Collinson L and Engel BD (2024) Integrating cellular electron microscopy with multimodal data to explore biology across space and time. *Cell* **187**(3), 563–584. https://doi.org/10.1016/J.CELL.2024.01.005

McDonald K, Schwarz H, Müller-Reichert T, Webb R, Buser C and Morphew M (2010) "Tips and tricks" for high-pressure freezing of model systems. *Methods in Cell Biology* **96**(C), 671–693. https://doi.org/10.1016/S0091-679X(10)96028-7

McDowall AW, Chang J-J, Freeman R, Lepault J, Walter CA and Dubochet J (1983) Electron microscopy of frozen hydrated sections of vitreous ice and vitrified biological samples. *Journal of Microscopy* **131**(1), 1–9. https://doi.org/10.1111/J.1365-2818.1983.TB04225.X

Medeiros JM, Böck D, Weiss GL, Kooger R, Wepf RA and Pilhofer M (2018) Robust workflow and instrumentation for cryo-focused ion beam milling of samples for electron cryotomography. *Ultramicroscopy* **190**, 1–11. https://doi.org/10.1016/J.ULTRAMIC.2018.04.002

Melia CE and Bharat TAM (2018) Locating macromolecules and determining structures inside bacterial cells using electron cryotomography. *Biochimica et Biophysica Acta* **1866**(9), 973. https://doi.org/10.1016/J.BBAPAP.2018.06.003

Moebel E, Martinez-Sanchez A, Lamm L, Righetto RD, Wietrzynski W, Albert S, Larivière D, Fourmentin E, Pfeffer S, Ortiz J, Baumeister W, Peng T, Engel BD and Kervrann C (2021) Deep learning improves macromolecule identification in 3D cellular cryo-electron tomograms. *Nature Methods* **18**(11), 1386–1394. https://doi.org/10.1038/s41592-021-01275-4

Moor H (1987) Theory and practice of high pressure freezing. *Cryotechniques in Biological Electron Microscopy*, 175–191. https://doi.org/10.1007/978-3-642-72815-0_8

Moor H and Riehle U (1968) Snap-freezing under high pressure: a new fixation technique for freeze-etching. In Bocciarelli S (ed.), *Proceedings of 4th European Regional Conference on Electron Microscopy*, 33–34.

Müller H, Jin J, Danev R, Spence J, Padmore H and Glaeser RM (2010) Design of an electron microscope phase plate using a focused continuous-wave laser. *New Journal of Physics* **12**. https://doi.org/10.1088/1367-2630/12/7/073011

Neselu K, Wang B, Rice WJ, Potter CS, Carragher B and Chua EYD (2023) Measuring the effects of ice thickness on resolution in single particle cryo-EM. *Journal of Structural Biology X* **7**, 100085. https://doi.org/10.1016/J.YJSBX.2023.100085

Nguyen HTD, Perone G, Klena N, Vazzana R, Kaluthantrige Don F, Silva M, Sorrentino S, Swuec P, Leroux F, Kalebic N, Coscia F and Erdmann PS (2024) Serialized on-grid lift-in sectioning for tomography (SOLIST) enables a biopsy at the nanoscale. *Nature Methods* **21**(9), 1693–1701. https://doi.org/10.1038/s41592-024-02384-6

Ni T, Sun Y, Burn W, Al-Hazeem MMJ, Zhu Y, Yu X, Liu LN and Zhang P (2022) Structure and assembly of cargo Rubisco in two native α-carboxysomes. *Nature Communications* **13**(1), 1–9. https://doi.org/10.1038/s41467-022-32004-w

Noble AJ and de Marco A (2024) Cryo-focused ion beam for in situ structural biology: State of the art, challenges, and perspectives. *Current Opinion in Structural Biology* **87**. https://doi.org/10.1016/J.SBI.2024.102864

Nogales E and Mahamid J (2024) Bridging structural and cell biology with cryo-electron microscopy. *Nature* **628**(8006), 47–56. https://doi.org/10.1038/s41586-024-07198-2

Nogales E and Scheres SHW (2015) Cryo-EM: A unique tool for the visualization of macromolecular complexity. *Molecular Cell* **58**(4), 677–689. https://doi.org/10.1016/J.MOLCEL.2015.02.019

Obr M, Keizer J, Righetto R, Zhang X, Kelley R, Khavnekar S, Franken E, Engel B, Plitzko J and Kotecha A (2024) Cryo-electron tomography of *Chlamydomonas reinhardtii*: Leveraging electron event representation (EER) image format in visual proteomics. *Microscopy and Microanalysis* **30**(Supplement_1). https://doi.org/10.1093/MAM/OZAE044.363

Ochner H and Bharat TAM (2023) Charting the molecular landscape of the cell. *Structure*, **31**(11) 1297–1305. https://doi.org/10.1016/J.STR.2023.08.015

Oikonomou CM, Chang YW and Jensen GJ (2016) A new view into prokaryotic cell biology from electron cryotomography. *Nature Reviews Microbiology* **14**(4), 205–220. https://doi.org/10.1038/NRMICRO.2016.7

O'Reilly FJ, Xue L, Graziadei A, Sinn L, Lenz S, Tegunov D, Blötz C, Singh N, Hagen WJH, Cramer P, Stülke J, Mahamid J and Rappsilber J (2020) In-cell architecture of an actively transcribing-translating expressome. *Science* **369**(6503), 554. https://doi.org/10.1126/SCIENCE.ABB3758

Otón J, Pereiro E, Conesa JJ, Chichón FJ, Luque D, Rodríguez JM, Pérez-Berná AJ, Sorzano COS, Klukowska J, Herman GT, Vargas J, Marabini R, Carrascosa JL and Carazo JM (2017) XTEND: Extending the depth of field

https://doi.org/10.1017/S0033583525000010 Published online by Cambridge University Press

in cryo soft X-ray tomography. *Scientific Reports* **7**(1), 1–12. https://doi.org/10.1038/srep45808

Parkhurst JM, Crawshaw AD, Siebert CA, Dumoux M, Owen CD, Nunes P, Waterman D, Glen T, Stuart DI, Naismith JH and Evans G (2023) Investigation of the milling characteristics of different focused-ion-beam sources assessed by three-dimensional electron diffraction from crystal lamellae. *IUCrJ* **10**(Pt 3), 270–287. https://doi.org/10.1107/S2052252523001902

Passarelli MK, Pirkl A, Moellers R, Grinfeld D, Kollmer F, Havelund R, Newman CF, Marshall PS, Arlinghaus H, Alexander MR, West A, Horning S, Niehuis E, Makarov A, Dollery CT and Gilmore IS (2017) The 3D OrbiSIMS—Label-free metabolic imaging with subcellular lateral resolution and high mass-resolving power. *Nature Methods* **14**(12), 1175–1183. https://doi.org/10.1038/nmeth.4504

Peck A, Carter SD, Mai H, Chen S, Burt A and Jensen GJ (2022) Montage electron tomography of vitrified specimens. *Journal of Structural Biology* **214**(2), 107860. https://doi.org/10.1016/J.JSB.2022.107860

Pegg DE (2007) Principles of cryopreservation. *Methods in Molecular Biology* **368**, 39–57. https://doi.org/10.1007/978-1-59745-362-2_3

Petrov PN, Müller H and Glaeser RM (2022) Perspective: Emerging strategies for determining atomic-resolution structures of macromolecular complexes within cells. *Journal of Structural Biology* **214**(1), 107827. https://doi.org/10.1016/J.JSB.2021.107827

Plitzko JM, Klumpe S, Schioetz OH, Bieber A, Capitanio C, Kuba J and Rigort A (2022) On the road to correlative cryo-lift-out, fully automated waffles and beyond – Make the most out of your tissue sample. *Microscopy and Microanalysis* **28**(S1), 1292–1295. https://doi.org/10.1017/S143192762200530X

Pyle E, Miller EA and Zanetti G (2024) Cryo-electron tomography reveals how COPII assembles on cargo-containing membranes. *Nature Structural & Molecular Biology*, 1–7. https://doi.org/10.1038/s41594-024-01413-4

Ravelli RBG, Nijpels FJT, Henderikx RJM, Weissenberger G, Thewessem S, Gijsbers A, Beulen BWAMM, López-Iglesias C and Peters PJ (2020) Cryo-EM structures from sub-nl volumes using pin-printing and jet vitrification. *Nature Communications* **11**(1), 1–9. https://doi.org/10.1038/s41467-020-16392-5

Rice G, Wagner T, Stabrin M, Sitsel O, Prumbaum D and Raunser S (2023) TomoTwin: Generalized 3D localization of macromolecules in cryo-electron tomograms with structural data mining. *Nature Methods* **20**(6), 871–880. https://doi.org/10.1038/S41592-023-01878-Z

Rigort A, Bäuerlein FJB, Villa E, Eibauer M, Laugks T, Baumeister W and Plitzko JM (2012) Focused ion beam micromachining of eukaryotic cells for cryoelectron tomography. *Proceedings of the National Academy of Sciences of the United States of America* **109**(12), 4449–4454. https://doi.org/10.1073/PNAS.1201333109

Rigort A and Plitzko JM (2015) Cryo-focused-ion-beam applications in structural biology. *Archives of Biochemistry and Biophysics* **581**, 122–130. https://doi.org/10.1016/J.ABB.2015.02.009

Rigort A, Villa E, Bäuerlein FJB, Engel BD and Plitzko JM (2012) Integrative approaches for cellular cryo-electron tomography: Correlative imaging and focused ion beam micromachining. *Methods in Cell Biology* **111**, 259–281. https://doi.org/10.1016/B978-0-12-416026-2.00014-5

Rubino S, Akhtar S, Melin P, Searle A, Spellward P and Leifer K (2012) A site-specific focused-ion-beam lift-out method for cryo transmission electron microscopy. *Journal of Structural Biology* **180**(3), 572–576. https://doi.org/10.1016/J.JSB.2012.08.012

dos Santos Á, Knowles O, Dendooven T, Hale T, Hale VL, Burt A, Kolata P, Cannone G, Bellini D, Barford D and Allegretti M (2024) Human spermatogenesis leads to a reduced nuclear pore structure and function. *BioRxiv*, 2024.10.30.620797. https://doi.org/10.1101/2024.10.30.620797

Schaffer M, Mahamid J, Engel BD, Laugks T, Baumeister W and Plitzko JM (2017) Optimized cryo-focused ion beam sample preparation aimed at in situ structural studies of membrane proteins. *Journal of Structural Biology* **197**(2), 73–82. https://doi.org/10.1016/J.JSB.2016.07.010

Schaffer M, Pfeffer S, Mahamid J, Kleindiek S, Laugks T, Albert S, Engel BD, Rummel A, Smith AJ, Baumeister W and Plitzko JM (2019) A cryo-FIB lift-out technique enables molecular-resolution cryo-ET within native *Caenorhabditis elegans* tissue. *Nature Methods* **16**(8), 757–762. https://doi.org/10.1038/S41592-019-0497-5

Scher N, Rechav K, Paul-Gilloteaux P and Avinoam O (2021) In situ fiducial markers for 3D correlative cryo-fluorescence and FIB-SEM imaging. *IScience* **24**(7), 102714. https://doi.org/10.1016/j.isci.2021.102714

Schertel A, Snaidero N, Han HM, Ruhwedel T, Laue M, Grabenbauer M and Möbius W (2013) Cryo FIB-SEM: Volume imaging of cellular ultrastructure in native frozen specimens. *Journal of Structural Biology* **184**(2), 355–360. https://doi.org/10.1016/J.JSB.2013.09.024

Schiøtz OH, Kaiser CJO, Klumpe S, Morado DR, Poege M, Schneider J, Beck F, Klebl DP, Thompson C and Plitzko JM (2023) Serial lift-out: Sampling the molecular anatomy of whole organisms. *Nature Methods*, 1–9. https://doi.org/10.1038/s41592-023-02113-5

Schur FKM, Obr M, Hagen WJH, Wan W, Jakobi AJ, Kirkpatrick JM, Sachse C, Kräusslich HG and Briggs JAG (2016) An atomic model of HIV-1 capsid-SP1 reveals structures regulating assembly and maturation. *Science* **353**(6298), 506–508. https://doi.org/10.1126/SCIENCE.AAF9620

Schwartz O, Axelrod JJ, Campbell SL, Turnbaugh C, Glaeser RM and Müller H (2019) Laser phase plate for transmission electron microscopy. *Nature Methods* **16**(10), 1016–1020. https://doi.org/10.1038/s41592-019-0552-2

Singh D, Soni N, Hutchings J, Echeverria I, Shaikh F, Duquette M, Suslov S, Li Z, van Eeuwen T, Molloy K, Shi Y, Wang J, Guo Q, Chait BT, Fernandez-Martinez J, Rout MP, Sali A and Villa E (2024) The molecular architecture of the nuclear basket. *BioRxiv*, 2024.03.27.587068. https://doi.org/10.1101/2024.03.27.587068

Studer D, Humbel BM and Chiquet M (2008) Electron microscopy of high pressure frozen samples: Bridging the gap between cellular ultrastructure and atomic resolution. *Histochemistry and Cell Biology* **130**(5), 877–889. https://doi.org/10.1007/S00418-008-0500-1

Sviben S, Gal A, Hood MA, Bertinetti L, Politi Y, Bennet M, Krishnamoorthy P, Schertel A, Wirth R, Sorrentino A, Pereiro E, Faivre D and Scheffel A (2016) A vacuole-like compartment concentrates a disordered calcium phase in a key coccolithophorid alga. *Nature Communications* **7**(1), 1–9. https://doi.org/10.1038/ncomms11228

Tacke S, Erdmann P, Wang Z, Klumpe S, Grange M, Plitzko J and Raunser S (2021) A streamlined workflow for automated cryo focused ion beam milling. *Journal of Structural Biology* **213**(3), 107743. https://doi.org/10.1016/J.JSB.2021.107743

Tegunov D, Xue L, Dienemann C, Cramer P and Mahamid J (2021) Multi-particle cryo-EM refinement with M visualizes ribosome-antibiotic complex at 3.5 Å in cells. *Nature Methods* **18**(2), 186–193. https://doi.org/10.1038/s41592-020-01054-7

Tamborrini D, Wang Z, Wagner T, Tacke S, Stabrin M, Grange M, Lin Kho A, Rees, M, Bennett P, Gautel M, Raunser, S. Structure of the native myosin filament in the relaxed cardiac sarcomere. *Nature* **623**, 863–871 (2023). https://doi.org/10.1038/s41586-023-06690-5

Tuijtel MW, Cruz-León S, Kreysing JP, Welsch S, Hummer G, Beck M and Turoňová B (2024) Thinner is not always better: Optimizing cryo-lamellae for subtomogram averaging. *Science Advances* **10**(17) https://doi.org/10.1126/SCIADV.ADK6285

Turoňová B, Sikora M, Schürmann C, Hagen WJH, Welsch S, Blanc FEC, von Bülow S, Gecht M, Bagola K, Hörner C, van Zandbergen G, Landry J, de Azevedo NTD, Mosalaganti S, Schwarz A, Covino R, Mühlebach MD, Hummer G, Locker JK and Beck M (2020) In situ structural analysis of SARS-CoV-2 spike reveals flexibility mediated by three hinges. *Science* **370**(6513), 203–208. https://doi.org/10.1126/SCIENCE.ABD5223

Uchida M, McDermott G, Wetzler M, Le Gros MA, Myllys M, Knoechel C, Barron AE and Larabell CA (2009) Soft X-ray tomography of phenotypic switching and the cellular response to antifungal peptoids in *Candida albicans*. *Proceedings of the National Academy of Sciences of the United States of America* **106**(46), 19375. https://doi.org/10.1073/PNAS.0906145106

Vidavsky N, Akiva A, Kaplan-Ashiri I, Rechav K, Addadi L, Weiner S and Schertel A (2016) Cryo-FIB-SEM serial milling and block face imaging: Large volume structural analysis of biological tissues preserved close to their native state. *Journal of Structural Biology* **196**(3), 487–495. https://doi.org/10.1016/J.JSB.2016.09.016

Vidavsky N, Masic A, Schertel A, Weiner S and Addadi L (2015) Mineral-bearing vesicle transport in sea urchin embryos. *Journal of Structural Biology* **192**(3), 358–365. https://doi.org/10.1016/J.JSB.2015.09.017

Villa E, Schaffer M, Plitzko JM and Baumeister W (2013) Opening windows into the cell: Focused-ion-beam milling for cryo-electron tomography. *Current Opinion in Structural Biology* **23**(5), 771–777. https://doi.org/10.1016/J.SBI.2013.08.006

von Kügelgen A, Cassidy CK, Van Dorst S, Pagani LL, Batters C, Ford Z, Löwe J, Alva V, Stansfeld PJ and Tanmay Bharat AM (2024) Membraneless channels sieve cations in ammonia-oxidizing marine archaea. *Nature*, 1–7. https://doi.org/10.1038/s41586-024-07462-5

von Kügelgen A, Tang H, Hardy GG, Kureisaite-Ciziene D, Brun YV, Stansfeld PJ, Robinson CV and Bharat TAM (2020) In situ structure of an intact lipopolysaccharide-bound bacterial surface layer. *Cell* **180**(2), 348. https://doi.org/10.1016/J.CELL.2019.12.006

Wagner FR, Watanabe R, Schampers R, Singh D, Persoon H, Schaffer M, Fruhstorfer P., Plitzko J and Villa E (2020) Preparing samples from whole cells using focused-ion-beam milling for cryo-electron tomography. *Nature Protocols* **15**(6), 2041–2070. https://doi.org/10.1038/s41596-020-0320-x

Wagner J, Carvajal AI, Bracher A, Beck F, Wan W, Bohn S, Körner R, Baumeister W, Fernandez-Busnadiego R and Hartl FU (2024) Visualizing chaperonin function in situ by cryo-electron tomography. *Nature* **633**(8029), 459–464. https://doi.org/10.1038/s41586-024-07843-w

Wagner T, Lusnig L, Pospich S, Stabrin M, Schonfeld F and Raunser S (2020) Two particle-picking procedures for filamentous proteins: SPHIRE-crYOLO filament mode and SPHIRE-STRIPER. *Acta Crystallographica Section D: Structural Biology* **76**(7), 613–620. https://doi.org/10.1107/S2059798320007342

Wagner T, Merino F, Stabrin M, Moriya T, Antoni C, Apelbaum A, Hagel P, Sitsel O, Raisch T, Prumbaum D, Quentin D, Roderer D, Tacke S, Siebolds B, Schubert E, Shaikh TR, Lill P, Gatsogiannis C and Raunser S (2019) SPHIRE-crYOLO is a fast and accurate fully automated particle picker for cryo-EM. *Communications Biology* **2**(1), 1–13. https://doi.org/10.1038/s42003-019-0437-z

Waltz F, Righetto RD, Kelley R, Zhang X, Obr M, Khavnekar S, Kotecha A and Engel BD (2024) In-cell architecture of the mitochondrial respiratory chain. *BioRxiv*, 2024.09.03.610704. https://doi.org/10.1101/2024.09.03.610704

Wan W, Khavnekar S and Wagner J (2024) STOPGAP: An open-source package for template matching, subtomogram alignment and classification. *Acta Crystallographica Section D Structural Biology* **80**(5), 336–349. https://doi.org/10.1107/S205979832400295X

Wang S, Zhou H, Chen W, Jiang Y, Yan X, You H and Li X (2023) CryoFIB milling large tissue samples for cryo-electron tomography. *Scientific Reports* **13**(1), 1–12. https://doi.org/10.1038/s41598-023-32716-z

Wang Z, Grange M, Pospich S, Wagner T, Kho AL, Gautel M and Raunser S (2022) Structures from intact myofibrils reveal mechanism of thin filament regulation through nebulin. *Science* **375**(6582) https://doi.org/10.1126/science.abn1934

Wang Z, Grange M, Wagner T, Kho AL, Gautel M and Raunser S (2021) The molecular basis for sarcomere organization in vertebrate skeletal muscle. *Cell* **184**(8), 2135. https://doi.org/10.1016/J.CELL.2021.02.047

Watanabe R, Buschauer R, Böhning J, Audagnotto M, Lasker K, Lu TW, Boassa D, Taylor S and Villa E (2020) The in situ structure of Parkinson's disease-linked LRRK2. *Cell* **182**(6), 1508–1518.e16. https://doi.org/10.1016/J.CELL.2020.08.004

Watanabe R, Zyla D, Parekh D, Hong C, Jones Y, Schendel SL, Wan W, Castillon G and Saphire EO (2024) Intracellular Ebola virus nucleocapsid assembly revealed by in situ cryo-electron tomography. *Cell* **187**(20), 5587–5603.e19. https://doi.org/10.1016/J.CELL.2024.08.044

Weil MT, Ruhwedel T, Meschkat M, Sadowski B and Möbius W (2019) Transmission electron microscopy of oligodendrocytes and myelin. *Methods in Molecular Biology* **1936**, 343–375. https://doi.org/10.1007/978-1-4939-9072-6_20

Weiner A, Kapishnikov S, Shimoni E, Cordes S, Guttmann P, Schneider G and Elbaum M (2013) Vitrification of thick samples for soft X-ray cryo-tomography by high pressure freezing. *Journal of Structural Biology* **181**(1), 77–81. https://doi.org/10.1016/J.JSB.2012.10.005

Weiß D, Schneider G, Niemann B, Guttmann P, Rudolph D and Schmahl G (2000) Computed tomography of cryogenic biological specimens based on X-ray microscopic images. *Ultramicroscopy* **84**(3–4), 185–197. https://doi.org/10.1016/S0304-3991(00)00034-6

Wieferig JP, Mills DJ and Kühlbrandt W (2021) Devitrification reduces beam-induced movement in cryo-EM. *IUCrJ* **8**(2), 186–194. https://doi.org/10.1107/S2052252520016243

Wolf SG and Elbaum M (2019) CryoSTEM tomography in biology. *Methods in Cell Biology* **152**, 197–215. https://doi.org/10.1016/BS.MCB.2019.04.001

Wolf SG, Houben L and Elbaum M (2014) Cryo-scanning transmission electron tomography of vitrified cells. *Nature Methods* **11**(4), 423–428. https://doi.org/10.1038/nmeth.2842

Wolf SG, Mutsafi Y, Dadosh T, Ilani T, Lansky Z, Horowitz B, Rubin S, Elbaum M and Fass D (2017) 3D visualization of mitochondrial solid-phase calcium stores in whole cells. *ELife* **6**. https://doi.org/10.7554/ELIFE.29929

Wozny MR, Di Luca A, Morado DR, Picco A, Khaddaj R, Campomanes P, Ivanović L, Hoffmann PC, Miller EA, Vanni S and Kukulski W (2023) In situ architecture of the ER–mitochondria encounter structure. *Nature* **618**(7963), 188–192. https://doi.org/10.1038/s41586-023-06050-3

Xu CS, Hayworth KJ, Lu Z, Grob P, Hassan AM, García-Cerdán JG, Niyogi KK, Nogales E, Weinberg RJ and Hess HF (2017) Enhanced FIB-SEM systems for large-volume 3D imaging. *ELife* **6**. https://doi.org/10.7554/ELIFE.25916

Xu CS, Pang S, Shtengel G, Müller A, Ritter AT, Hoffman HK, ya Takemura S, Lu Z, Pasolli HA, Iyer N, Chung J, Bennett D, Weigel AV, Freeman M, van Engelenburg SB, Walther TC, Farese RV, Lippincott-Schwartz J, Mellman I, … Hess HF (2021) An open-access volume electron microscopy atlas of whole cells and tissues. *Nature* **599**(7883), 147–151. https://doi.org/10.1038/s41586-021-03992-4

Xue L, Lenz S, Zimmermann-Kogadeeva M, Tegunov D, Cramer P, Bork P, Rappsilber J and Mahamid J (2022) Visualizing translation dynamics at atomic detail inside a bacterial cell. *Nature* **610**(7930), 205–211. https://doi.org/10.1038/s41586-022-05255-2

Yang JE, Larson MR, Sibert BS, Kim JY, Parrell D, Sanchez JC, Pappas V, Kumar A, Cai K, Thompson K and Wright ER (2023) Correlative montage parallel array cryo-tomography for in situ structural cell biology. *Nature Methods* **20**(10), 1537–1543. https://doi.org/10.1038/s41592-023-01999-5

Yang J, Vrbovská V, Franke T, Sibert B, Larson M, Coomes T, Rigort A, Mitchels J and Wright E R. (2023) Precise 3D localization by integrated fluorescence microscopy (iFLM) for cryo-FIB-milling and in-situ cryo-ET. *Microscopy and Microanalysis* (Supplement_1), 1055–1057. https://doi.org/10.1093/MICMIC/OZAD067.541

You X, Zhang X, Cheng J, Xiao Y, Ma J, Sun S, Zhang X, Wang HW and Sui SF (2023) In situ structure of the red algal phycobilisome–PSII–PSI–LHC megacomplex. *Nature* **616**(7955), 199–206. https://doi.org/10.1038/s41586-023-05831-0

Zachs T, Schertel A, Medeiros J, Weiss GL, Hugener J, Matos J and Pilhofer M (2020) Fully automated, sequential focused ion beam milling for cryo-electron tomography. *ELife* **9**. https://doi.org/10.7554/ELIFE.52286

Zens B, Fäßler F, Hansen JM, Hauschild R, Datler J, Hodirnau V-V, Zheden V, Alanko J, Sixt M and Schur FKM (2024) Lift-out cryo-FIBSEM and cryo-ET reveal the ultrastructural landscape of extracellular matrix. *Journal of Cell Biology* **223**(6) https://doi.org/10.1083/JCB.202309125

Zhang J, Zhang D, Sun L, Ji G, Huang X, Niu T, Xu J, Ma C, Zhu Y, Gao N, Xu W and Sun F (2021) VHUT-cryo-FIB, a method to fabricate frozen hydrated lamellae from tissue specimens for in situ cryo-electron tomography. *Journal of Structural Biology* **213**(3), 107763. https://doi.org/10.1016/J.JSB.2021.107763

Zhang P (2019) Advances in cryo-electron tomography and subtomogram averaging and classification. *Current Opinion in Structural Biology*, **58** 249–258. https://doi.org/10.1016/J.SBI.2019.05.021

Zhang X, Sridharan S, Zagoriy I, Eugster Oegema C, Ching C, Pflaesterer T, Fung HKH, Becher I, Poser I, Müller CW, Hyman AA, Savitski MM and Mahamid, J (2023) Molecular mechanisms of stress-induced reactivation in mumps virus condensates. *Cell* **186**(9), 1877–1894.e27. https://doi.org/10.1016/J.CELL.2023.03.015

Zheng S, Wolff G, Greenan G, Chen Z, Faas FGA, Bárcena M, Koster AJ, Cheng Y and Agard DA (2022) AreTomo: An integrated software package for automated marker-free, motion-corrected cryo-electron tomographic alignment and reconstruction. *Journal of Structural Biology: X* **6**, 100068. https://doi.org/10.1016/J.YJSBX.2022.100068

Zhong X, **Wade CA**, **Withers PJ**, **Zhou X**, **Cai C**, **Haigh SJ and Burke MG** (2021) Comparing Xe+pFIB and Ga+FIB for TEM sample preparation of Al alloys: Minimising FIB-induced artefacts. *Journal of Microscopy* **282**(2), 101. https://doi.org/10.1111/JMI.12983

Zimmerli CE, **Allegretti M**, **Rantos V**, **Goetz SK**, **Obarska-Kosinska A**, **Zagoriy I**, **Halavatyi A**, **Hummer G**, **Mahamid J**, **Kosinski J and Beck M** (2021) Nuclear pores dilate and constrict in cellulo. *Science* **374**(6573) https://doi.org/10.1126/science.abd9776

Zivanov J, **Otón J**, **Ke Z**, **von Kügelgen A**, **Pyle E**, **Qu K**, **Morado D**, **Castaño-Díez D**, **Zanetti G**, **Bharat TA**, **Briggs JA and Scheres SH** (2022) A Bayesian approach to single-particle electron cryo-tomography in RELION-4.0. *ELife* **11**. https://doi.org/10.7554/ELIFE.83724

https://doi.org/10.1017/S0033583525000010 Published online by Cambridge University Press